ENHANCEMENT OF Q AND K² IN $AL_{0.8}SC_{0.2}N$/GAN/SAPPHIRE SURFACE ACOUSTIC WAVE RESONATORS USING SEMICONDUCTOR GROUND CONTACT

Yue Zheng[1], Jialin Wang[1], Mingyo Park[1], Ping Wang[2], Ding Wang[2], Zetian Mi[2] and Azadeh Ansari[1]
[1]Georgia Institute of Technology, Atlanta GA, USA
[2]University of Michigan, Ann Arbor MI 48109, USA

ABSTRACT

This work reports on the super high frequency (SHF) surface acoustic wave (SAW) resonators with bottom ground contact, based on 200 nm-thick epitaxial aluminum scandium nitride ($Al_{0.8}Sc_{0.2}N$) on gallium nitride (GaN)/sapphire with high doped n-GaN as the bottom electrode. $Al_{0.8}Sc_{0.2}N$ epitaxial films are grown on GaN/sapphire template with molecular beam epitaxy (MBE). Interdigital transducers with a pitch size of 0.4 µm are patterned with electron beam lithography (EBL). By taking advantage of a grounded bottom semiconductor contact and the high acoustic velocity of Sezawa modes, a four-time improvement of Q value from 172 to 819 is attained at a resonance frequency of 5.792 GHz.

KEYWORDS

Sezawa mode; Aluminum Scandium Nitride; Gallium Nitride; Surface acoustic wave; Molecular Beam Epitaxy; Super High Frequency; Quality factor; Ground Contact.

INTRODUCTION

Surface acoustic wave (SAW) resonators made of piezoelectric materials are well known for offering a low-loss and low-cost solution for RF bandpass filter applications owing to the advantage of high-temperature stability and non-releasing fabrication technique [1], [2]. In order to construct SAW resonators with high quality (Q) factor and high electromechanical coupling coefficient (K^2), it is essential to grow a piezoelectric film with an ordered lattice structure and fewer crystallographic defects, particularly when the device is scaled down to target super high frequency (SHF) band required by 5G/6G standards [3]. As a novel piezoelectric material, aluminum scandium nitride ($Al_{1-x}Sc_xN$) deposited by DC magnetron sputtering method can suffer from low growth quality, particularly when the Sc composition is high: abnormally oriented grains can be formed if the $Al_{1-x}Sc_xN$ lattice is mismatched with the growth template [4].

Gallium Nitride (GaN), a wide bandgap piezoelectric material with hexagonal wurtzite structure, is nearly lattice-matched with $Al_{1-x}Sc_xN$ [5]. Besides its applications in piezoelectric transducers, GaN is a versatile material that is promising for on-chip integration of multi-functional III-nitride devices [6]. *In situ* silicon (Si)-doped GaN can serve as a conductive interface [7]. Acoustoelectric amplifiers with DC voltage tuning can be made by harnessing the phonon-electron interaction in unintentionally doped (UID) GaN [8]. With the ability to form two-dimensional electron gas (2DEG), AlGaN/GaN heterostructure is commonly utilized for high mobility electron transistor (HEMT) [9]. With epitaxial $Al_{1-x}Sc_xN$ grown on GaN template, it is possible to leverage the above advantages to control $Al_{1-x}Sc_xN$-based transducers.

In our previous work, we demonstrated ferroelectric polarization switching and fabricated one-port SAW resonators with floating Si-GaN bottom on two separate $Al_{0.8}Sc_{0.2}N$/GaN/sapphire devices [10], [11]. Multiple Sezawa modes operating at 3-6 GHz with moderately high Q factor were probed in this structure, offering a multi-band high-frequency solutions to radio frequency (RF) filters. However, to observe both functionalities on the same device, the Si-GaN bottom contact layer needs to be grounded. Therefore, it is necessary to investigate the effect of bottom contact on the performance of the SAW resonator.

The electrostatic boundary conditions of the bottom contact and the normalized thickness (h/λ) of the piezoelectric film both affect the K^2 of SAW modes and lamb-wave (LW) modes due to the change of static capacitance (C_o) and piezoelectric coefficient under different applied electric field [12], [13]. SAW and LW resonators with small h/λ (< 0.5) with grounded bottom electrodes are reported to enhance the K^2 but usually come at a price of increased feedthrough level and degraded Q factor [13]–[15]. The impact of metal bottom electrode has been thoroughly investigated in the past; however, the role of a semiconductor ground on resonator performance has not been well understood.

In this work, we report on the first demonstration of two-port $Al_{0.8}Sc_{0.2}N$/GaN/sapphire SAW resonator employing n-type Si-doped GaN as a semiconductor bottom contact. The growth quality of $Al_{1-x}Sc_xN$ is controlled by using (1) GaN as a growth template and (2) molecular beam epitaxy (MBE) to grow textured $Al_{1-x}Sc_xN$ epitaxial thin film. We remove the piezoelectric film under the signal probing region to reduce undesired resonance and parasitic capacitance caused by probing pads. Compared to the SAW resonators with floated bottom contact, the device with grounded bottom contact achieves a boost of Q by 376% and a slight improvement of effective mechanical coupling coefficient (k_{eff}^2) for both Rayleigh (R) and Sezawa (S) modes.

DEVICE STRUCTURE AND FABRICATION PROCESS

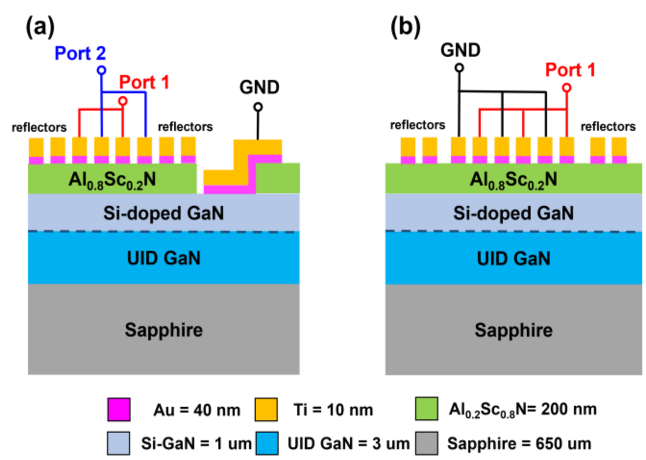

Figure 1: Schematic cross section view of (a) 2-port $Al_{0.8}Sc_{0.2}N$/GaN/Sapphire SAW resonator with grounded GaN contact, and (b) 1-port SAW resonator with floated bottom contact.

We previously reported the fabrication of one-port SAW resonators with 0.4 µm – 0.6 µm pitch sizes and floating Si-GaN bottom contact (Fig. 1(b)). The growth techniques of the $Al_{0.8}Sc_{0.2}N$-on-GaN/sapphire film, the fabrication process of the one-port SAW devices and the RF characterization methods were described in [16] and [10], and hence will not be repeated.

Fig. 2 (a) shows the high-resolution transmission electron microscopy (HRTEM) of the $Al_{0.8}Sc_{0.2}N$/GaN/sapphire film for the fabrication of SAW resonators. The rocking curve (Fig. 2(b)) and the 2theta-omega (2θ/ω) scan (Fig. 2(c)) from X-ray diffraction (XRD) shows a full width at half maximum (FWHM) of 300 arcseconds for the $Al_{0.8}Sc_{0.2}N$ layer.

In this work, we fabricate two-port 0.4 μm-pitched SAW resonators with grounded n-GaN contact (Fig. 1(a)). To access the n-GaN bottom contact (BC), the $Al_{0.8}Sc_{0.2}N$ is etched by inductively coupled plasma (ICP), and conformal Ti/Au coating is subsequently deposited with RF sputtering method. To reduce the high electrical feedthrough level observed in the previous work, we etch the $Al_{0.8}Sc_{0.2}N$ area under the signal probing pads to remove the parasitic capacitance and fill with 200 nm of SiO_2 deposited by electron beam evaporation. Fig. 2(d) shows the scanning electron microscope (SEM) image of the 0.4 μm-pitched two-port SAW resonator, and the inset shows the close-up detail of the interdigital transducer (IDT) structure.

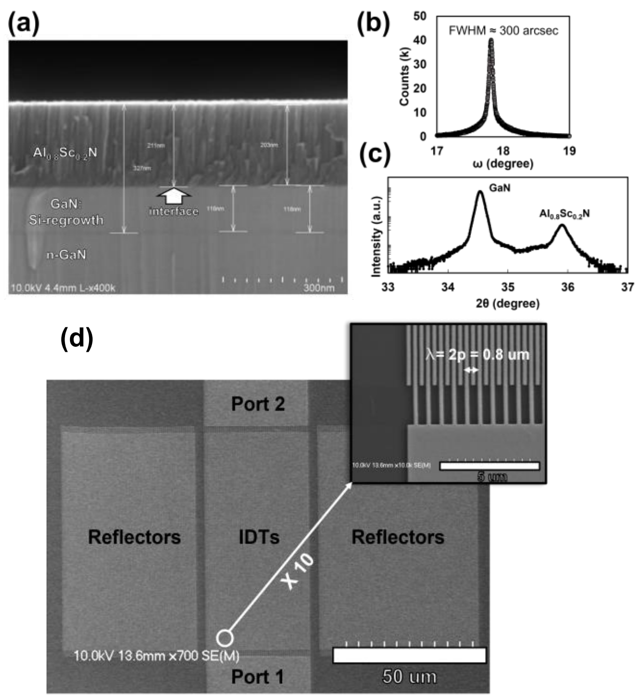

Figure 2. (a) HRTEM image showing the cross-sectional morphology of epitaxial $Al_{0.8}Sc_{0.2}N$ on GaN. (b) Rocking curve and (c) (002) plane XRD 2θ/ω scan of $Al_{0.8}Sc_{0.2}N$/GaN. (d) SEM image of a fabricated 2-port SAW resonator with a 400 nm pitch size. Inset shows the zoomed-in view of the IDT fingers and the bus line.

DEVICE CHARACTERIZATION AND EXPERIMENTAL RESULTS

Characterization of SAW Resonators with Grounded Contact

The frequency response of the SAW devices was measured using Keysight N5224B PNA microwave network analyzer. Fig. 3 illustrates the evaluated tested electromechanical performance of the SAW devices, including floated and grounded BC.

Fig. 3(a) and Fig. 3 (b) present the wideband input admittance (Y_{11}) response and the transfer admittance (Y_{12}) response of the two-port 0.4 μm-pitched SAW resonators with grounded BC. The Y_{11} response from the previous devices (with floated BC) is plotted for comparison. k_{eff}^2 of each mode is determined using [17]:

$$k_{eff}^2 = \frac{\pi^2}{4}(f_p - f_s)\frac{f_s}{f_p^2}, \qquad (1)$$

where f_s is the series resonance frequency and f_p is the parallel resonance frequency.

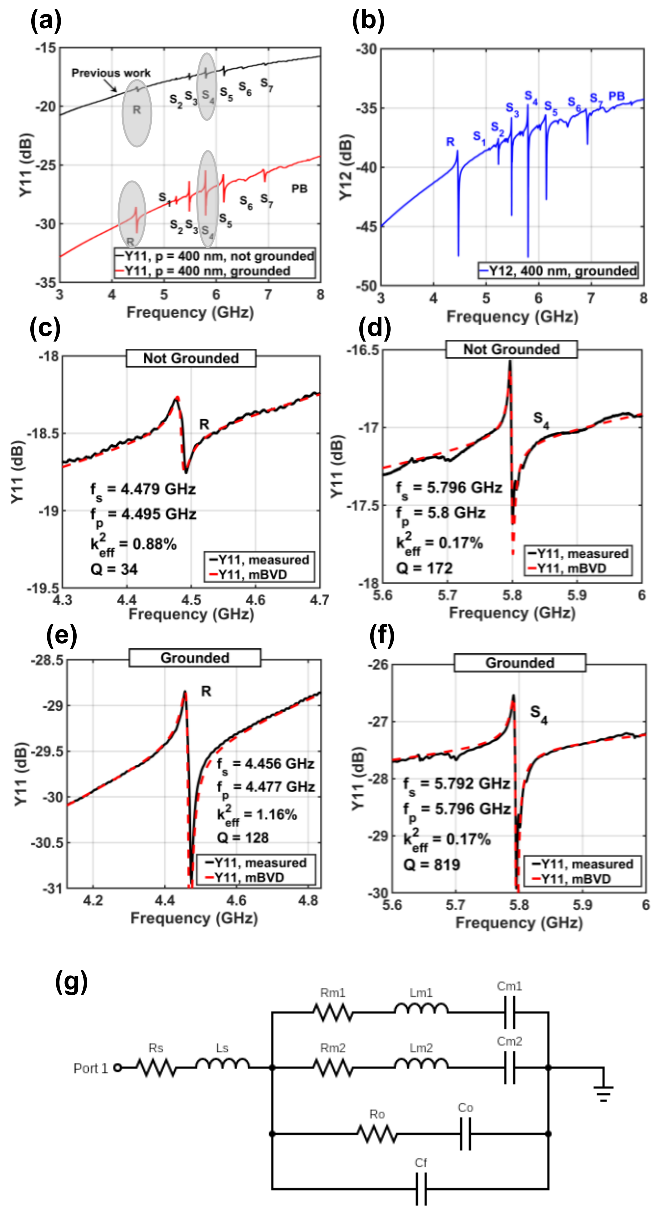

Figure 3. (a) Measured wideband Y_{11} response of the 0.4 μm-pitch $Al_{0.8}Sc_{0.2}N$/GaN/Sapphire SAW resonators with and without grounding the Si-doped GaN surface. (b) Y_{12} response of the resonator with grounded contact. Zoomed-in peak with mBVD fitting of R mode and S_4 mode from the Y_{11} response of SAW resonator (c)-(d) with floated bottom contact and (e)-(f) with grounded contact. (g) Modified Butterworth Van Dyke (mBVD) circuit model for Y_{11} characteristics fitting.

The Bode quality factor (Q_{Bode}) is extracted from S-parameters, according to [18]:

$$Q_{bode}=\omega\times\tau_g(\omega)\frac{|S_{11}|}{(1-|S_{11}|)^2}, \quad (2)$$

where ω is the angular frequency (rad/s) and τ_g is the group delay. The highest Q_{bode} exhibited in the two-port resonator is 819 from the fourth-order Sezawa (S_4) mode at 5.792 GHz. Table 1 compares the measured f_s, f_p, k_{eff}^2 and Q factor of R and S_4 modes with grounded and floated resonator BC.

It can be noticed that the grounded BC has minimal impact on the resonance frequencies. For S_4 mode, a four-time improvement of Q is achieved with grounded BC, showing a Q value of 819 at a resonance frequency of 5.792 GHz. The enhancement of the Q factor could be caused by a shift of the electrical potential profile in GaN layer, as it has been shown that Q can be amplified under the acoustoelectric effect by tuning the potential level in GaN layer [19]. Removal of the piezoelectric film under signal probing pads contribute to the decrease of feedthrough level and may also aid the Q factor enhancement.

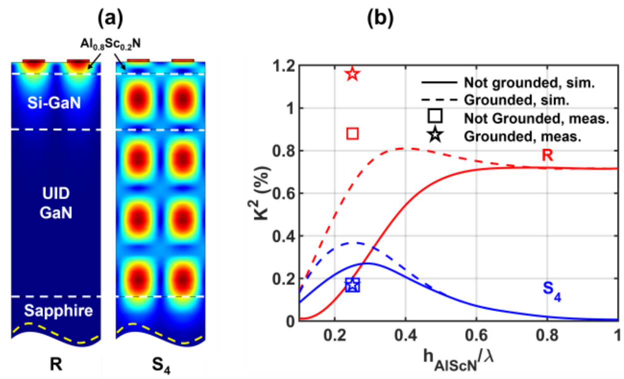

Figure 4. COMSOL simulated (a) 2-D cross-sectional displacement field of Rayleigh (R) mode and fourth-order Sezawa (S_4) mode, and (b) dispersion relations of the electromechanical coupling coefficient (K^2) with respect to the normalized AlScN thickness (h_{AlScN}/λ); marked stars/squares show the measured values for the devices.

In order to study the contribution of bottom ground contact to the electromechanical coupling, finite element modeling (FEM) of the fabricated device is constructed on the scale of one acoustic wavelength (λ) using COMSOL Multiphysics®. The K^2 is assessed by [20]:

$$K^2=2\times\frac{v_{oc}-v_{sc}}{v_{oc}}, \quad (3)$$

where v_{oc} and v_{sc} are the phase velocities when the surface boundary condition of the $Al_{0.8}Sc_{0.2}N$ is open-circuited (free) and short-circuited (grounded) respectively [21]. The relative dielectric permittivity ϵ_r of 13.7 is used for $Al_{0.8}Sc_{0.2}N$ in the simulation [22]. It should be noted that the dielectric property of the thin film is subjected to the residual strain level induced at different growth temperatures, and the actual value ϵ_r of in the AlScN film might be different from the literature value. Fig. 4(a) shows the mode shape of R and S_4 modes of the resonator with 0.4 µm pitch size. Fig. 4(b) compares the dispersion relations of the K^2 of the resonator with grounded and floating electrostatic boundary condition at the AlScN/GaN interface, showing the K^2 enhancement for a normalized thickness (h_{AlScN}/λ) less than 0.6. The K^2 enhancement is due to the improved d_{33} coupling in $Al_{0.8}Sc_{0.2}N$ in the presence of a vertical electric field. It should be noted that the K^2 values of R mode from simulations are smaller than the measured k_{eff}^2 values, which is also reported in [23]. The reason for such underprediction could also be attributed to an overestimation of ϵ_r of $Al_{0.8}Sc_{0.2}N$ at high frequency, as it has been reported that at high frequency, ϵ_r degrades to half of the low-frequency value for aluminum nitride [24].

Table 1. Summary of f, k_{eff}^2 and Q values from the measurements of the 0.4 µm-pitched SAW devices.

Mode	Bottom Contact	f_s (GHz)	f_p (GHz)	k_{eff}^2	Q_{Bode}
R	Not grounded	4.479	4.495	0.88%	34
	grounded	4.456	4.477	1.16%	128
S_4	Not grounded	5.796	5.800	0.17%	172
	grounded	5.792	5.796	0.17%	819

Frequency Response of SAW Resonators with mBVD Model

To further understand the enhancement mechanisms of k_{eff}^2 and Q factor in the resonators with grounded BC, the measured results of R mode and S_4 mode are fitted by the modified Butterworth-Van Dyke (mBVD) circuit model [25]. The model is made of a series RLC circuit (R_m, L_m and C_m) that represents the motional branch of each acoustic resonance and a static capacitance C_0 and a resistance R_0 that model the capacitance between IDT fingers and resistive loss in electrodes (Fig. 3 (g)). An additional feedback capacitance C_f is included to model the UID-GaN film capacitance [26]. R_s and L_s account for the parasitic effect caused by the probing pads to improve impedance matching. The unloaded quality factor Q_m can be extracted using the fitted motional branch circuit component values using:

$$Q_m=\frac{1}{R_m}\sqrt{\frac{L_m}{C_m}}. \quad (4)$$

Fig. 3(c)-(f) show the zoomed-in peaks of R modes and S_4 modes corresponding to each SAW resonator, along with the fitted response using the mBVD model. Table 2 summarizes the mBVD parameters and the evaluated Q_m of R and S_4 modes of the SAW resonators with/without grounding the BC.

Table 2. Summary of the mBVD parameters used to fit the 0.4 µm-pitched SAW devices with/without the grounded BC.

Mode	Bottom Contact	C_o (pF)	C_f (pF)	C_m (fF)	L_m (nH)	R_m (Ω)	Q_m
R	Not grounded	98	5.35	1.22	1029	72	403
	grounded	803	1.22	1.06	1198	74	454
S_4	Not grounded	98	5.35	0.8	941	22	1558
	grounded	803	1.22	0.53	1437	22	2366

CONCLUSION

In this paper, we demonstrate the enhancement of Q and k_{eff}^2 of a multi-mode AlScN/GaN/sapphire SAW resonator with grounded n-GaN contact operating from 3-6 GHz. $Al_{0.8}Sc_{0.2}N$ epitaxial film is grown with the MBE method on a lattice-matched GaN/sapphire template to ensure good film quality. By utilizing the grounded n-

GaN contact and minimizing the parasitic capacitance, the largest enhancement of *Q* factor occurs in S_4 mode, whose *Q* value features a four-time improvement from 172 to 819. We verify the role of the grounded bottom contact on K^2 and *Q* factor with COMSOL FEM and mBVD model. This work demonstrates the versatility of GaN on a single device and facilitates future investigation on DC tuning of the SAW resonator.

REFERENCES

[1] K. Hashimoto, "RF Bulk acoustic wave filters for communications," p. 275, 2009.

[2] Y. Y. Chen, C. M. Lin, and T. T. Wu, "A novel weighted method for wide-band SAW filters using slanted finger interdigital transducers on layered piezoelectric substrates," Proc. - IEEE Ultrason. Symp., vol. 4, pp. 2182–2185, 2005.

[3] A. Bogner, R. Bauder, H.-J. Timme, T. Forster, C. Reccius, R. Weigel, and A. M. Hagelauer, "Enhanced Piezoelectric $Al_{1-x}Sc_xN$ RF-MEMS Resonators for Sub-6 GHz RF-Filter Applications: Design, Fabrication and Characterization," Proc. IEEE Int. Conf. Micro Electro Mech. Syst., pp. 1258–1261, 2020.

[4] C. S. Sandu, F. Parsapour, S. Mertin, V. Pashchenko, R. Matloub, T. LaGrange, B. Heinz, and P. Muralt, "Abnormal Grain Growth in AlScN Thin Films Induced by Complexion Formation at Crystallite Interfaces," Phys. Status Solidi Appl. Mater. Sci., vol. 216, no. 2, Jan. 2019.

[5] P. Wang, D. Wang, N. M. Vu, T. Chiang, J. T. Heron, and Z. Mi, "Fully epitaxial ferroelectric ScAlN grown by molecular beam epitaxy," Appl. Phys. Lett., vol. 118, no. 22, pp. 1–6.

[6] M. Rais-Zadeh, V. J. Gokhale, A. Ansari, M. Faucher, D. Théron, Y. Cordier, and L. Buchaillot, "Gallium nitride as an electromechanical material," J. Microelectromechanical Syst., vol. 23, no. 6, pp. 1252–1271, Dec. 2014.

[7] Y. Arakawa, K. Ueno, H. Imabeppu, A. Kobayashi, J. Ohta, and H. Fujioka, "Electrical properties of Si-doped GaN prepared using pulsed sputtering," Appl. Phys. Lett., vol. 110, no. 4, p. 042103, Jan. 2017.

[8] V. J. Gokhale and M. Rais-Zadeh, "Phonon-Electron Interactions in Piezoelectric Semiconductor Bulk Acoustic Wave Resonators," Sci. Reports 2014 41, vol. 4, no. 1, pp. 1–10, Jul. 2014.

[9] U. K. Mishra, P. Parikh, and Y. F. Wu, "AlGaN/GaN HEMTs - An overview of device operation and applications," Proc. IEEE, vol. 90, no. 6, pp. 1022–1031, 2002.

[10] Y. Zheng, J. Wang, M. Park, P. Wang, D. Wang, Z. Mi, and A. Ansari, "High-Order Sezawa Mode AlScN/GaN/Sapphire Surface Acoustic Wave Resonators," IEEE MEMS, pp. 1046–1049, 2022.

[11] D. Wang, P. Wang, B. Wang, and Z. Mi, "Fully epitaxial ferroelectric ScGaN grown on GaN by molecular beam epitaxy," Appl. Phys. Lett., vol. 119, no. 11, p. 111902, Sep. 2021.

[12] G. Tang, "Investigation on High Performance Surface Acoustic Wave Devices Using ScAlN Thin Films," 2017.

[13] M. Park and A. Ansari, "Epitaxial $Al_{0.77}Sc_{0.23}N$ SAW and Lamb Wave Resonators," IFCS-ISAF 2020 - Jt. Conf. IEEE Int. Freq. Control Symp. IEEE Int. Symp. Appl. Ferroelectr. Proc., Jul. 2020.

[14] A. Qamar, M. Jafari, and M. Rais-Zadeh, "Solidly mounted anti-symmetric lamb-wave delay lines as an alternate to SAW devices," IEEE Electron Device Lett., vol. 39, no. 12, pp. 1916–1919, Dec. 2018.

[15] C. M. Lin, V. Yantchev, J. Zou, Y. Y. Chen, and A. P. Pisano, "Micromachined one-port aluminum nitride lamb wave resonators utilizing the lowest-order symmetric mode," J. Microelectromechanical Syst., vol. 23, no. 1, pp. 78–91, Feb. 2014.

[16] P. Wang, D. A. Laleyan, A. Pandey, Y. Sun, and Z. Mi, "Molecular beam epitaxy and characterization of wurtzite $Sc_xAl_{1-x}N$," Appl. Phys. Lett., vol. 116, no. 15, p. 151903, Apr. 2020.

[17] H. Campanella, "Acoustic wave and electromechanical resonators : concept to key applications," p. 345, 2010.

[18] D. A. Feld, R. Parker, R. Ruby, P. Bradley, and S. Dong, "After 60 years: A new formula for computing quality factor is warranted," in Proceedings - IEEE Ultrasonics Symposium, 2008, pp. 431–436.

[19] V. J. Gokhale, Y. Shim, and M. Rais-Zadeh, "Observation of the acoustoelectric effect in gallium nitride micromechanical bulk acoustic filters," 2010 IEEE Int. Freq. Control Symp. FCS 2010, pp. 524–529, 2010.

[20] K. Yamanouchi and T. Ishii, "High temperature stable acoustic surface wave substrates of $SiO_2/LiNbO_3$ structure with super high coupling," Japanese J. Appl. Physics, Part 1 Regul. Pap. Short Notes Rev. Pap., vol. 41, no. 5 B, pp. 3480–3482, May 2002.

[21] J. Zou, C. M. Lin, A. Gao, and A. P. Pisano, "The multi-mode resonance in AlN lamb wave resonators," J. Microelectromechanical Syst., vol. 27, no. 6, pp. 973–984, Dec. 2018.

[22] G. Wingqvist, F. Tasnádi, A. Zukauskaite, J. Birch, H. Arwin, and L. Hultman, "Increased electromechanical coupling in w-$Sc_xAl_{1-x}N$," Appl. Phys. Lett., vol. 97, no. 11, pp. 95–98, 2010.

[23] Z. Hao, M. Park, D. Kim, A. Clark, R. Dargis, H. Zhu, and A. Ansari, "Single Crystalline ScAlN Surface Acoustic Wave Resonators with Large Figure of Merit ($Q\times k_t^2$)," 2019 IEEE MTT-S International Microwave Symposium (IMS), pp. 786–789, 2019.

[24] A. T. Collins, E. C. Lightowlers, and P. J. Dean, "Lattice Vibration Spectra of Aluminum Nitride," Phys. Rev., vol. 158, no. 3, p. 833, Jun. 1967.

[25] J. D. Larson, P. D. Bradley, S. Wartenberg, and R. C. Ruby, "Modified Butterworth-Van Dyke circuit for FBAR resonators and automated measurement system," Proc. IEEE Ultrason. Symp., vol. 1, pp. 863–868, 2000.

[26] Y. Wang, W. Goh, K. Chai, X. Mu, Y. Hong, P. Kropenlnicki, and M. Je, "Parasitic analysis and π-type Butterworth-Van Dyke model for complementary-metal-oxide-semiconductor Lamb wave resonator with accurate two-port Y-parameter characterizations," Rev. Sci. Instrum., vol. 87, no. 4, p. 045004, Apr. 2016.

CONTACT

*Yue Zheng, Georgia Institute of Technology,
Atlanta, GA 30332; Email: yzheng331@gatech.edu

*Azadeh Ansari, Georgia Institute of Technology,
Atlanta, GA 30332; Email: azadeh.ansari@ece.gatech.edu